DOI: 10.1021/ic901976y

Inorganic Chemistry
Article

An Experimental Solution to the "Missing Hydrogens" Question Surrounding the Macropolyhedral 19-Vertex Boron Hydride Monoanion $[B_{19}H_{22}]^-$, a Simplification of Its Synthesis, and Its Use As an Intermediate in the First Example of *syn*-$B_{18}H_{22}$ to *anti*-$B_{18}H_{22}$ Isomer Conversion

Michael G. S. Londesborough,*,† Jonathan Bould,*,†,‡ Tomáš Baše,† Drahomír Hnyk,† Mario Bakardjiev,† Josef Holub,† Ivana Císařová,§ and John D. Kennedy‡

†*Institute of Inorganic Chemistry v.v.i., Academy of Sciences of the Czech Republic, Řež by Prague, 250 68, Czech Republic,* ‡*Department of Chemistry, University of Leeds, Leeds, LS6 9JT, United Kingdom, and* §*Faculty of Natural Science, Charles University, Hlavova 2030, 128 43, Prague 2, Czech Republic*

Received October 6, 2009

The macropolyhedral $[B_{19}H_{22}]^-$ monoanion **1** and the dianion $[B_{19}H_{21}]^{2-}$ **2** are synthesized in consistent 86−92% yields by the reaction of $[PSH]^+[syn\text{-}B_{18}H_{21}]^-$ with $BH_3(SMe_2)$ in 1,2-$Cl_2C_2H_4$ at 72 °C. ['PS' is an abbreviation for 'Proton Sponge', 1,8-bis-(dimethylamino)naphthalene. 'PSH' is its protonated derivative.] The molecular structures of **1** and **2** were elucidated as their $[PS\{BH_2\}]^+$ and $[PS\{BH_2\}]_2^+$ salts **1a** and **2a** by single-crystal X-ray diffraction studies, in which all atoms were located, and supported by mass spectrometric analyses together with calculations of the cluster molecular geometries (ab ignitio and/or DFT) and of ^{11}B chemical shifts based on GIAO−DFT shielding tensors. Acidification of dianion **2** with CF_3COOH in acetonitrile, H_2SO_4 in dichloromethane, or aqueous HCl results in the clean formation of the monoanion $[B_{19}H_{22}]^-$ **1**. Conversely, shaking a concentrated acetonitrile solution of **1** in 0.5 M aqueous NaOH cleanly yields the $[B_{19}H_{21}]^{2-}$ dianion **2**. Reaction of a dichloromethane solution of **1** with a 36% aqueous solution of HCHO in the presence of H_2SO_4 quantitatively converts **1** at room temperature to a 1:1 mixture of the *syn*- and *anti*-isomers of $B_{18}H_{22}$. This cluster dismantling process is the first example of a *syn*- to *anti*-$B_{18}H_{22}$ isomer conversion.

Introduction

The development of the full potential of boron-containing cluster chemistry requires the development of cluster architectures larger than the 12-boron icosahedron.[1] The high molecular boron content and stability of such species make them commercially interesting compounds for several applications in, for example, medicine[2−4] and materials.[2,5−8] The rapid expansion of boron-containing cluster chemistry in the 1960s and early 1970s resulted in the description of $B_{13}H_{19}$,[9] $B_{14}H_{18}$,[10] $B_{14}H_{20}$,[11] $B_{15}H_{23}$,[12] $B_{16}H_{20}$,[13] and the *syn* and *anti* isomers of $B_{18}H_{22}$[14] and $B_{20}H_{16}$,[15,16] all resulting from the intimate cluster fusion of smaller borane clusters. Further binary boron hydride cluster structural motifs have subsequently been rare and essentially limited to $B_{12}H_{16}$ and its conjugate $[B_{12}H_{15}]^-$ anion,[17] the $[B_{22}H_{22}]^{2-}$ anion,[18,19] the

*To whom correspondence should be addressed. E-mail: michaell@iic.cas.cz (M.G.S.L.), jbould@gmail.com (J.B.).

(1) Shea, S. L.; Bould, J.; Londesborough, M. G. S.; Perera, S. D.; Franken, A.; Ormsby, D. L.; Jelínek, T.; Stíbr, B.; Holub, J.; Kilner, C. A.; Thornton-Pett, M.; Kennedy, J. D. *Pure Appl. Chem.* **2003**, *75*, 1239.
(2) Plešek, J. *Chem. Rev.* **1992**, *92*, 269.
(3) Hawthorne, M. F. *Angew. Chem., Int. Ed.* **1993**, *32*, 950.
(4) Soloway, A. H.; Tjarks, W.; Barnum, B. A.; Rong, F. G.; Barth, R. F.; Codogni, I. M.; Wilson, J. G. *Chem. Rev.* **1998**, *98*, 1515.
(5) Lu, X.; Shao, L.; Wang, X.; Chen, Q.; Liu, J.; Chu, W. K.; Bennet, J.; Ling, P. *Proc. Electrochem. Soc.* **2001**, *2001*, 337–344.
(6) Kawasaki, Y.; Kuroi, T.; Yamashita, T.; Horita, K. H., T.; Ishibashi, M.; Togawa, M.; Ohno, Y.; Yoneda, M.; Horsky, T.; Jacobson, D.; Krull, W. A. *Nucl. Instrum. Methods Phys. Res., Sect. B* **2005**, *237*, 25.
(7) Heo, S.; Hwang, H.; Cho, H. T.; Krull, W. A. *Appl. Phys. Lett.* **2006**, 89.
(8) Harris, M. A.; Huynh, C. *Solid State Technol.* **2007**, *50*, 33.
(9) Huffman, J. C.; Moody, D. C.; Schaeffer, R. *Inorg. Chem.* **1976**, *15*, 227.
(10) Heřmánek, S.; Fetter, K.; Plešek, J.; Todd, L. J.; Garber, A. R. *Inorg. Chem.* **1975**, *14*, 2250.
(11) Huffman, J. C.; Moody, D. C.; Schaeffer, R. *J. Am. Chem. Soc.* **1975**, *97*, 1621.
(12) Rathke, J.; Schaeffer, R. *Inorg. Chem.* **1974**, *13*, 3008.
(13) Plešek, J.; Heřmánek, S.; Hanoušek, F. *Collect. Czech. Chem. Commun.* **1968**, *33*, 699.
(14) Olsen, F. P.; Vasavada, R. C.; Hawthorne, M. F. *J. Am. Chem. Soc.* **1968**, *90*, 3946.
(15) Friedman, L. B.; Dobrott, R. D.; Lipscomb, W. N. *J. Am. Chem. Soc.* **1963**, *85*, 3505.
(16) Miller, N. E.; Muetterties, E. L. *J. Am. Chem. Soc.* **1963**, *85*, 3506.
(17) Brewer, C. T.; Swisher, R. G.; Sinn, E.; Grimes, R. N. *J. Am. Chem. Soc.* **1985**, *107*, 3558.
(18) Volkov, O.; Dirk, W.; Englert, U.; Paetzold, P. *Z. Anorg. Allg. Chem.* **1999**, *625*, 1193.
(19) Hosmane, N. S.; Franken, A.; Zhang, G. M.; Srivastava, R. R.; Smith, R. Y.; Spielvogel, B. F. *Main Group Met. Chem.* **1998**, *21*, 319.

Published on Web 03/29/2010

[*fac*-$B_{20}H_{18}$]$^{2-}$ and [$B_{21}H_{18}$]$^{-}$ anions,[20] and two species previously identified as the [$B_{19}H_{20}$]$^{-}$ monoanion and its conjugate [$B_{19}H_{19}$]$^{2-}$ dianion, reported in 2000.[21] The [$B_{19}H_{20}$]$^{-}$ empirical formula given[21] to the first of these 19-vertex cluster species by Dopke et al. was subsequently questioned[22] by Jemmis et al., who proposed, on the basis of DFT calculations, that the [$B_{19}H_{20}$]$^{-}$ formulation was missing two hydrogen atoms and did therefore not fit into their *mno* rules for fused borane clusters.[23] Although Jemmis et al. did not suggest the location of these hydrogen atoms from the DFT calculations, Kiani and Hofmann subsequently proposed[24] a molecular structure for the monoanion based on calculations. Considering the limited number of cluster types available in the boron hydride structural continuum, particularly in the larger "macropolyhedral" category, it is important to experimentally certify those postulated by theory and calculation. In this contribution, we present clear experimental evidence confirming the macropolyhedral 19-vertex boron hydride anions in question as being [$B_{19}H_{22}$]$^{-}$ and [$B_{19}H_{21}$]$^{2-}$, and our X-ray diffraction, NMR spectroscopic, and calculation studies reasonably locate the positions of all hydrogen atoms.

Results and Discussion

The ready synthesis[14,25−27] and stability of both *syn* and *anti* isomers of $B_{18}H_{22}$ make them a convenient starting point for advanced investigation of large-molecule boron hydrides. In this context, Dopke et al. showed that the reaction of [*anti*-$B_{18}H_{20}$]$^{2-}$ with $BH_2Cl(SMe_2)$ or $BHCl_2(SMe_2)$ produces a 19-boron anion, which they proposed to be of formulation [$B_{19}H_{20}$]$^{-}$, in *ca.* 70% yield. However, their reported procedure requires the use of vacuum line techniques, rigorously dried solvents, and difficult-to-handle potassium hydride. Moreover, in our hands, this method has proved to be unreliable with inconsistent yields. We have now found that a simple stirring of warm 1,2-dichloroethane solutions of *syn*-$B_{18}H_{22}$ and 1,8-bis-(dimethylamino)naphthalene together with the nonhalogenated $BH_3(SMe_2)$ followed by simple filtration affords the [$B_{19}H_{22}$]$^{-}$ (**1**) and [$B_{19}H_{21}$]$^{2-}$ (**2**) anions in consistent yields of 86−92%. The selective formation of **1** or **2** depends on the precise experimental conditions discussed below. Each is characterized by single-crystal X-ray diffraction analysis. A comparison of the ^{11}B NMR properties of anions **1** and **2** with the species synthesized by Dopke et al.[21] show them to be identical. However, our full structural characterizations now reveal the empirical formulas [$B_{19}H_{22}$]$^{-}$ and [$B_{19}H_{21}$]$^{2-}$, each with two more hydrogen atoms than proposed by those authors and now consistent with the suggestions by Jemmis et al.[22] and Kiani and Hofmann.[24] More specifically, the previously "missing" hydrogen atoms are now located experimentally. (See Scheme 1 for positions of cluster open-face hydrogen atoms for the originally published {$B_{19}H_{20}$}$^{-}$ as well as for anions **1** and **2**.)

Scheme 1

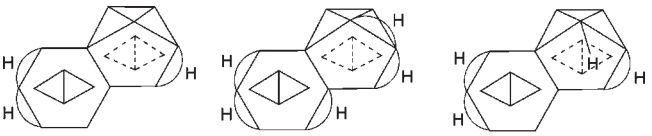

DFT and subsequent RMP2(fc) calculations [the terms R (restricted) and fc (frozen core) are in subsequent discussion omitted for simplicity] were carried out contemporaneously with the synthetic and crystallographic work in order to support the full structural characterization of the anions **1** and **2**. Figures 1 and 2 show both the crystallographically determined and the DFT-calculated molecular structures of **1** and **2**. Their shared overall macropolyhedral fused-cluster framework is notionally derived by the replacement of two bridging hydrogen atoms on the open face of one of the two 10-vertex *nido* subclusters in the 18-vertex *syn*-$B_{18}H_{22}$ by a {BH_2} moiety to form one *nido* 10-vertex subcluster and one *nido* 11-vertex subcluster with a shared two-atom B−B edge.

For the monoanion, **1**, the single-crystal X-ray diffraction study reveals 19 cluster boron atoms and 22 cluster hydrogen atoms. All hydrogen atoms connected to boron were located from the difference Fourier synthesis and were refined with isotropic thermal parameters. The structural calculations for **1** minimized energetically with five bridging hydrogen atoms, three on the 10-vertex subcluster and two on the 11-vertex subcluster, mirroring the configuration found in the crystal structure (Figure 1). Table 1 lists the calculated ^{11}B nuclear shieldings, expressed as ^{11}B NMR chemical shifts, together with the measured ^{11}B and ^{1}H-{^{11}B} chemical shift data for **1**. Table 2 lists selected calculated and measured interatomic dimensions for both **1** and **2**. The calculated and measured interatomic separations for **1** compare very well, with the majority of the calculated distances being within 0.015 Å of the experimental values. Exceptions are in the long edge of the 11-vertex subcluster, B(7)−B(11), where the calculated distance is longer by +0.025 Å, and the long edge in the 10-vertex subcluster, namely, B(7)−B(10′), +0.024 Å. More refined MP2/6-31G(d) calculations of the molecular geometry showed a slight improvement in these geometrical parameters to −0.011 and 0.020 Å respectively but with no decisive changes in the subsequent ^{11}B chemical shift values. That the calculated structures at the B3LYP/6-31+G(d,p) and MP2/6-31G(d) levels and methodologies represent good models of **1** may be taken from a consideration of the positions of the cluster bridging hydrogen atoms. Thus, the bridging hydrogen atoms spanning B(9)−B(10) and B-(10)−B(11) are quite unsymmetrical in both the calculated and the measured data with the distances to B(10) for μH(910) and μH(101) being 1.453 and 1.475 Å (calcd), which correspond well to the measured distances of 1.429(17) and 1.470(19) Å, respectively. A similar asymmetry is seen for the bridging hydrogen atom adjacent to the B(7′)−B(8) intercluster "hinge" atoms: μH(7′8) to B(8) is 1.383 (calcd), 1.470(19) Å (measd). The shorter arms for all three hydrogen atoms are in the range 1.239−1.282 (calcd) and 1.172-(18)−1.195(19) Å (measd). These asymmetries, tending toward an *endo*-terminal nature for the bridging hydrogen

(20) Bernhardt, E.; Brauer, D. J.; Finze, M.; Willner, H. *Angew. Chem., Int. Ed.* **2007**, *46*, 2927.
(21) Dopke, J. A.; Powell, D. R.; Gaines, D. F. *Inorg. Chem.* **2000**, *39*, 463.
(22) Jemmis, E. D.; Balakrishnarajan, M. M.; Pancharatna, P. D. *Inorg. Chem.* **2001**, *40*, 1730.
(23) Jemmis, E. D.; Balakrishnarajan, M. M.; Pancharatna, P. D. *Chem. Rev.* **2002**, *102*, 93.
(24) Kiani, F. A.; Hofmann, M. *Inorg. Chem.* **2006**, *45*, 6996.
(25) Adams, L.; Hosmane, S. N.; Eklund, J. E.; Wang, J.; Hosmane, N. S. *J. Am. Chem. Soc.* **2002**, *124*, 7292.
(26) Plešek, J.; Heřmánek, S.; Štíbr, B.; Hanoušek, F. *Collect. Czech. Chem. Commun.* **1967**, *32*, 1095.
(27) Li, Y.; Sneddon, L. G. *Inorg. Chem.* **2006**, *45*, 470.

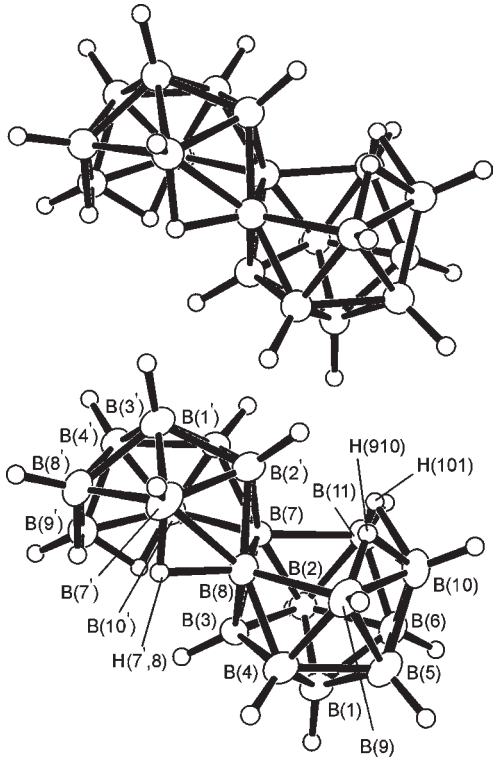

Figure 1. Lower diagram: Representation of the crystallographically determined molecular structure of the $[B_{19}H_{22}]^-$ anion **1** (50% probability thermal ellipsoids), as determined in its $[PS\{BH_2\}]^+$ salt **1a**, with the cation omitted to aid clarity. Upper diagram: The B3LYP/6-31+G(d,p) DFT calculated structure of **1**. Selected measured and calculated distances are shown in Table 2.

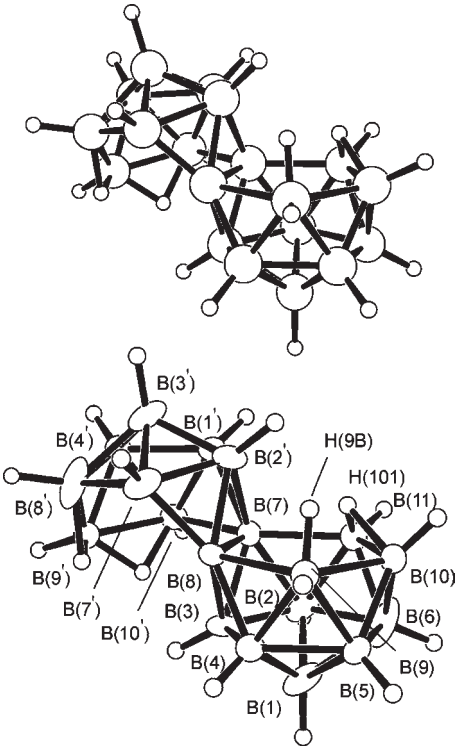

Figure 2. Lower diagram: Representation of the crystallographically determined molecular structure of the $[B_{19}H_{21}]^{2-}$ anion **2** (50% probability thermal ellipsoids), as determined in its $[PS\{BH_2\}]_2^+$ salt **2a**, with the cations omitted to aid clarity. Upper diagram: The B3LYP/6-31+G(d,p) DFT calculated structure of **2**. Selected measured and calculated distances are shown in Table 2.

atoms, are also apparent from B3LYP, MP2, and single-crystal X-ray studies of the single-cluster *nido*-$[B_{11}H_{14}]^-$ anion itself, in which the facial bridging and *endo*-terminal hydrogen atoms undergo rapid and unresolved fluxional exchange.[28a] By contrast, no fluxional behavior was observed in the proton spectrum for **1** between +80 and −39 °C, possibly due to a "fixing effect" of the replacement of an *endo*-terminal/bridging hydrogen atom on the open face of the $[B_{11}H_{14}]^-$ anion by the B(7)B(8) "intercluster hinge" in **1**. The majority of the ^{11}B NMR assignments for the calculated boron chemical shifts compare favorably with the assignments made by Dopke et al. from [^{11}B−^{11}B] COSY correlations.[21] Some assignments are switched, for example, B(5) and B(3) in Table 1, but these are only separated by 1 ppm, which is well below the precision expected for the GIAO-B3LYP method in these systems.

The $[B_{19}H_{21}]^{2-}$ dianion **2** was also isolated and initially identified by NMR spectroscopy by comparison with the ^{11}B NMR data reported by Dopke et al., who had proposed a $[B_{19}H_{19}]^{2-}$ formulation but who did not report a single-crystal X-ray diffraction study. In their work, dianion **2** was obtained by deprotonation of monoanion **1**, which we have confirmed to be $[B_{19}H_{22}]^-$; this suggests that the $[B_{19}H_{19}]^{2-}$ formulation given by Dopke et al. is also short by two hydrogen atoms. Our single-crystal X-ray diffraction study of **2** (Figure 2, lower diagram) confirms the 19 cluster boron atoms and now indeed shows 21 cluster hydrogen atoms. The proton removed by the base comes from the 10-vertex subcluster on the bridging position between B(8) and B(7′), confirming the proposal of Dopke et al. The 11-vertex subcluster features a bridging hydrogen atom spanning the B(10)−B(11) edge similar to that in the monoanion, but the asymmetry, which is apparent in the monoanion, is not evident here, either in the crystal structure or by calculation. The second open-face hydrogen atom, H(9B), exhibits a long distance of 1.92(4) Å measured (2.130/2.073 Å DFT/MP2 calcd) to the neighboring B(10) vertex and is thus tending toward an *endo*-terminal disposition, as may be found in the $[B_{11}H_{14}]^-$ anion.[28a] Overall, the experimentally observed bridging hydrogen atom characteristics are mirrored in the results of the structural calculations (Figure 2, upper diagram), with, in particular, the more symmetrical bridging nature of μH(10,11) and the substantial *endo* character of H(9B) being apparent in both cases.

The other measured and calculated interboron distances around the open face of the 11-vertex subcluster in **2** are reasonably in agreement, and the higher level MP2/6-31G(d) calculation does not substantially improve the match in most cases. Table 3 shows the calculated and measured ^{11}B NMR spectra for **2**. The tentative assignments for the boron resonances are based on a combination of GIAO-B3LYP/6-31+G(d,p) calculated chemical shifts and (^{11}B−^{11}B COSY), [^{1}H−^{1}H] COSY, and ^{1}H-{^{11}B selective} experiments. A high confidence in assignments suggested by COSY experiments is not warranted in this compound, which has a large proportion of its resonances very close together and overlapping. Additionally, the correspondence between the calculated and measured boron spectra is not as close as is the

(28) (a) Volkov, O.; Radacki, K.; Thomas, R. L.; Rath, N. P.; Barton, L. *J. Organomet. Chem.* **2005**, *690*, 2736. (b) Farràs, P.; Teixidor, F.; Branchadell, V. *Inorg. Chem.* **2006**, *45*, 7947.

Table 1. Measured $^{11}B-\{^1H\}$ Chemical Shifts Together with Calculated ^{11}B Chemical Shifts for the $[B_{19}H_{22}][PS\{BH_2\}]$ **1a**

tentative assignments[a]	lit.[b]	measured[c] $\delta(^{11}B)$ [$\delta(^1H)$]	calculated B3LYP/6-31+G(d,p) $\delta(^{11}B)$ [difference]
B(10′)	1′	+12.8[d] [+3.76]	+12.5 [−0.3]
B(3′)	3′	+12.8[e] [+3.59]	+12.0 [−0.8]
B(8)	7	−5.2 [singlet, −3.24 bridging H]	+3.8 [+7.0]
B(7)	8	+5.5 [singlet]	−4.3 [−9.8]
B(9′)	9′	−3.2 [+2.86]	−6.1 [−2.9]
B(4)	1	−5.2 [+2.29]	−7.2 [−2.0]
B(2)	4	−7.5 [+2.12]	−7.2 [+0.3]
B(10)	10	−7.5 [+2.21]	−8.8 [−1.3]
B(8′)	8′	−7.5 [+2.39]	−9.8 [−2.3]
B(1′)	10′	−7.5 [+2.59]	−10.4 [−2.9]
B(1)	2	−8.4 [+2.59]	−10.4 [−2.0]
B(9)	9	−18.6[f] [+2.10, $-1.88^{(2)}$]	−20.3 [−1.7]
B(11)	11	−21.2[g] [+0.65, $-2.41^{(2)}$]	−23.2 [−2.1]
B(2′)	2′	−21.9 [+1.46]	−22.7 [−0.9]
B(6)	6	−24.4 [+0.99]	−23.8 [+0.6]
B(5)	3	−25.4 [−0.87]	−25.2 [+0.2]
B(3)	5	−26.5 [+0.64]	−26.0 [+0.5]
B(7′)	7′	−27.7 [+1.69]	−28.6 [−0.9]
B(4′)	4′	−42.3 [−0.36]	−42.3 [0.0]
$H_2B.PS$ cation		+1.3[h] [+2.51]	+1.8 [−0.5]

[a] Assignments based on a combination of GIAO-B3LYP/6-31+G(d,p) calculated chemical shifts, $[^{11}B-^{11}B]$ COSY, and $^1H-\{^{11}B$ selective$\}$ experiments. [b] Assignments taken from ref 21. [c] Proton decoupled $\delta(^{11}B)$ chemical shifts measured in CD_3CN at 295 K. [d] $\delta(^{11}B)$ +13.1 ppm at 343 K. [e] $\delta(^{11}B)$ +12.2 ppm at 343 K. [f] Apparent doublet of doublets $^1J(^{11}B-^1H)$ 143 Hz, [x] $J(^{11}B-^1H)$ 49 Hz. [g] Unresolved coupling. [h] Triplet, $^1J(^{11}B-^1H)$ 120 Hz.

Table 2. Selected DFT Calculated and X-Ray Measured Interatomic Distances for $[B_{19}H_{22}][PS\{BH_2\}]$ **1a** and $[B_{19}H_{21}][PS\{BH_2\}]_2$ **2a**[a]

	monoanion, **1**		dianion, **2**		
	DFT	Meas.	DFT	MP2	Meas.
B(1) −B(2)	1.784	1.776(2)	1.790	1.782	1.787(5)
B(1) −B(3)	1.773	1.768(2)	1.748	1.748	1.763(5)
B(1) −B(4)	1.786	1.784(2)	1.806	1.796	1.805(5)
B(1) −B(5)	1.772	1.768(2)	1.769	1.764	1.795(5)
B(1) −B(6)	1.764	1.757(2)	1.784	1.776	1.813(6)
B(7) −B(8)	1.851	1.841(2)	1.817	1.828	1.848(4)
B(8) −B(9)	1.951	1.936(2)	2.190	2.114	2.090(5)
B(9) −B(10)	1.885	1.876(3)	1.987	1.961	1.933(5)
B(10) −B(11)	1.891	1.907(3)	1.836	1.826	1.938(5)
B(11) −B(7)	1.961	1.936(2)	1.981	1.943	1.942(4)
B(8)−B(7′)	1.863	1.851(2)	1.705	1.710	1.750(5)
B(7′)−B(8′)	1.930	1.934(2)	1.839	1.826	1.830(5)
B(7)−B(10′)	2.066	2.042(2)	2.169	2.085	2.146(5)
B(9′)−B(10′)	1.779	1.774(2)	1.824	1.766	1.823(5)
B(8′)−B(9′)	1.816	1.795(3)	1.772	1.806	1.819(6)
B(9)−H(910/9B)	1.240	1.170(17)	1.191	1.197	1.13(4)
H(910/9B)−B(10)	1.453	1.429(17)	2.130	2.073	1.92(4)
B(10)−H(101)	1.475	1.470(19)	1.342	1.345	1.41(4)
H(101)−B(11)	1.239	1.172(18)	1.286	1.284	1.26(4)
B(10′)−H(109)	1.333	1.268(17)	1.340	1.335	1.29(2)
H(109)−B(9′)	1.300	1.245(17)	1.302	1.300	1.30(3)
B(9′)−H(89′)	1.337	1.280(18)	1.327	1.329	1.26(3)
H(89′)−B(8′)	1.322	1.223(18)	1.329	1.335	1.49(3)
B(7′)−H(7′8)	1.282	1.195(19)			
H(7′8)−B(8)	1.383	1.470(19)			

[a] For a fuller listing of distances, see the Supporting Information.

case for the monoanion **1** (see Figure 3). Thus, it may be noted that the GIAO chemical shift values for the pair of resonances at the low-field end of the spectrum, $\delta(^{11}B)$ +12.8 ppm (assignment B(8)) and +12.8 ppm (assignment B(10′)), do not compare well with the DFT/MP2 calculated values of +24.0/+21.2 and +6.5/+4.9 ppm. Similarly, at the high-field end, the resonances appearing at −28.7 ppm (assignment B(6)) and −33.5 ppm (assignment B(4′)) differ considerably from the calculated values of −38.9/−15.7 and −41.9/−46.3 ppm. The attempts to model the system at the GIAO-B3LYP/II//MP2/6-31G(d) level do not decisively improve the comparison even though the overall calculated spectra, as seen in Figure 3, are similar. However, the calculations are, nevertheless, consistent with the experimentally determined structure, and they reveal the locations of all the open-face hydrogen atoms in reasonable positions as expected.

These latter considerations perhaps suggest that the methods of calculation may not constitute the origin of the discrepancy in the NMR data. A possible interpretation may be a subtle isomerization upon dissolution or perhaps fluxionality associated with the 11-vertex open face. In accord with the fluxionality of the bridging and *endo*-terminal hydrogen atoms of the $[B_{11}H_{14}]^-$ anion[28a] and other 11-vertex systems,[28b] a conversion in **2** of the *endo* hydrogen atom on B(9) to B(9)B(10) bridging character could be visualized as the B(10)B(11) bridging hydrogen atom concomitantly converted to BH(11) *endo* character. To test this, we carried out structural minimizations and calculations on species in which the BH(9) open-face hydrogen atom was fixed as *endo*, and then in which the other open-face hydrogen atom was fixed as *endo* on BH(11) instead. The first approximated closely to the global minimum for **2** and to the solid-state structure in **2a**, with shieldings close to the calculated values in Table 3. The second, with the open-face hydrogen atom fixed as *endo* on B(11), was found to be very close in energy, *ca.* 4.5 kJ mol^{-1} higher, which suggests that fluxionality could occur and that the observed population of the two forms would be essentially equal, and that mean shielding values would be observed if the barrier was low, which is reasonable. However, equal-weight averaging of the calculated boron nuclear shieldings for the two cases brought some, but not all, of the extreme chemical shifts more into line with those observed, but it also produced a bigger spread in the central region, indicating that, if such a fluxionality is involved, it is only part of the phenomenon (see Table 4 in the Supporting Information for a full list of calculated ^{11}B NMR chemical shifts).

Electrospray high resolution mass spectrometry gave the same spectrum for both **1a** and **2a**, consistent with $[B_{19}H_{22}]^-$. The spectrum shows, with the exception of a small amount of $[B_{18}H_{21}]^-$, no fragmentation of the nonadecaborate anion. Reversing the polarity of measurement provided the expected spectrum for the $[PS\{BH_2\}]^+$ cation in both cases.

In the synthesis of **1a** and **2a**, the choice of solvent was selected on the basis of polarity and boiling point: 1,2-dichloroethane holds all starting materials in solution, but the products conveniently precipitate, thereby facilitating their quick and simple isolation. Importantly, the boiling point of 1,2-$Cl_2C_2H_4$ is high enough to permit sufficient heating of the reaction mixture to boil off SMe_2 from its $\{BH_3\}$ adduct, thus liberating the reactive borane moiety. Through repeated experimentation, it became clear that the reaction temperature has an influence on the outcome of the synthesis. If the reaction mixture in 1,2-dichloroethane is brought to reflux temperature (83−84 °C), then, despite the fact that the course of reaction appears the same to the eye, the precipitated product is not compound **1a** or **2a** but instead $[B_{12}H_{12}][PSH]_2$. However, if the temperature of reaction is

Table 3. Measured $^{11}B-\{^1H\}$ Chemical Shifts Together with Calculated ^{11}B Chemical Shifts for the $[B_{19}H_{21}][PS\{BH_2\}]_2$ **2a**

tentative assignments[a]	lit.[b]	measured $\delta(^{11}B)[\delta(^1H)]$[a,c]	measured[b]	DFT [difference][d]	MP2
B(8)	8	+12.8 [singlet]	+13.6 (singlet)	+24.0 [+11.2]	+21.2
B(10′)	1′	+12.8 [+3.78, −1.84]	+11.8	+6.5 [−6.3]	+4.9
B(3′)	3′	−2.2 [+2.73]	−1.2	+0.5 [+2.7]	−0.6
B(1)	10	−3.2 [+2.35]	−3.2	−1.9 [+1.3]	−4.3
B(10)	1	−5.7 [+2.38]	−5.8	−5.0 [+0.7]	−5.6
B(7)	2	−7.3 [singlet]	−7.5	−5.2 [+1.5]	−16.9
B(2)	9′	−7.8 [+2.38]	−8.3	−9.6 [−1.8]	−20.6
B(11)	7	−8.8 [+2.55]	−9.3(singlet)	−10.3 [−1.5]	−14.9
B(5)	8′	−9.8 [+1.20]	−10.9	−12.3 [−2.5]	−41.4
B(9)	4	−11.6 [+1.95]	−12.1	−16.4 [−4.8]	−22.3
B(7′)	9	−18.0 [+1.94, −1.45]	−18.2	−16.5 [+1.5]	−18.9
B(8′)	11	−19.8 [+1.46, −2.67]	−19.5	−17.2 [+2.6]	−21.3
B(9′)	10′	−20.7 [+0.97, −3.62]	−20.1	−17.4 [+3.3]	−19.8
B(2′)	7′	−21.5 [−1.33]	−20.7	−18.2 [+3.3]	−17.7
B(4)	3	−22.2 [+1.78]	−21.8	−19.1 [+3.1]	−6.6
B(3)	5	−22.8 [+1.19]	−22.4	−20.0 [+2.8]	−22.2
B(1′)	2′	−23.5 [+1.55]	−22.7	−22.8 [+0.7]	−22.9
B(6)	6	−28.9 [+0.97]	−29.7	−38.9 [−10.0]	−15.7
B(4′)	4′	−33.5 [+0.66]	−35.2	−41.9 [−8.4]	−46.3
$H_2B.PS$ cation		+1.8 [+2.57]		+1.9 [+0.1]	

[a] Assignments based on a combination of GIAO-B3LYP/6-31+G[d,p] calculated chemical shifts and $^{11}B-^{11}B$ COSY, $[^1H-^1H]$ COSY, and $^1H-\{^{11}B$ selective} experiments [b] Data from ref 21. Recorded at 160.4 MHz, measured in CH_3CN, and referenced externally to $BF_3[OEt_2]$ in C_6D_6. [c] Measured in DMF-d^7. [d] Difference in the ^{11}B NMR chemical shifts between the calculated and measured data for this work.

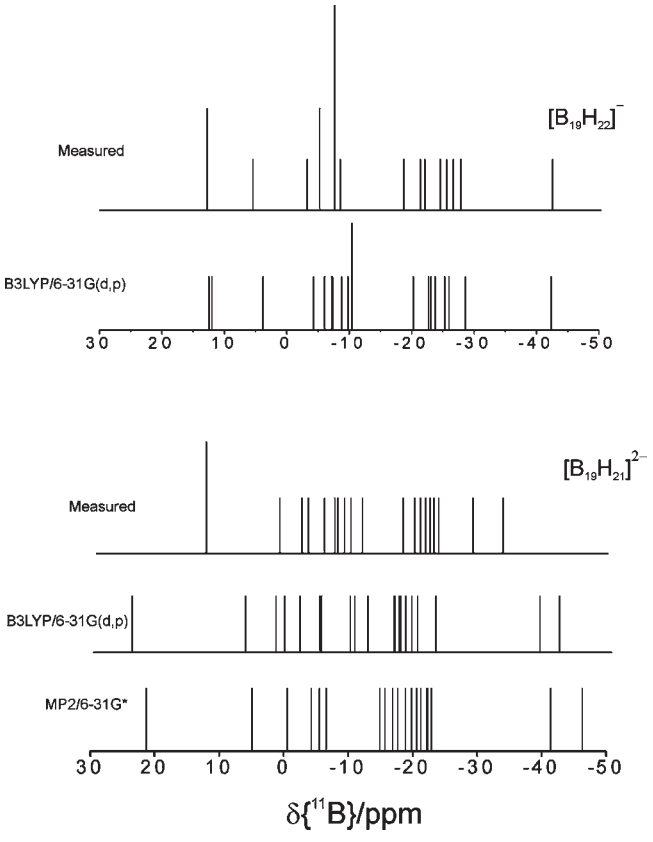

Figure 3. A stick diagram comparing the measured and the GIAO-B3LYP/6-31+G(d,p) calculated ^{11}B chemical shifts for the monoanion $[B_{19}H_{22}][PS\{BH_2\}]$ **1** (upper) and the measured GIAO-B3LYP/6-31+G(d,p) and GIAO-B3LYP/II//MP2/6-31G* calculated shifts for the dianion $[B_{19}H_{21}][PS\{BH_2\}]_2$ **2** (lower).

kept lower than 62 °C, then insertion of a boron vertex into the $\{B_{18}\}$ skeleton does not occur, and the $[B_{18}H_{21}][PSH]$ remains unchanged. In THF solvent, formation of $[B_{12}H_{12}][PSH]_2$ is favored over the production of **1a** and **2a**. A similar solvent sensitivity was noted by Dopke et al. in their route, where reactions carried out in THF produced no 19-vertex products and OEt_2 was the preferred solvent for 19-boron product formation. Finally, in the system we report here, it is of interest to note that *only* the *syn*-$B_{18}H_{22}$ isomer undergoes reaction with $BH_3(SMe_2)$. Under identical conditions, *anti*-$B_{18}H_{22}$ affords its conjugate dianion [*anti*-$B_{18}H_{20}]^{2-}$.

The monoanion and dianion may be easily interconverted. Thus, treatment of monoanion **1** with a base results in dianion **2**, and conversely, with acid, **2** reverts to the monoanion **1**. In the presence of H_2SO_4, the addition of a 36% aqueous HCHO to a solution of **1** in $CHCl_3$ leads to a fast and exothermic reaction affording an almost quantitative conversion to a 1:1 mixture of *syn* and *anti* isomers of $B_{18}H_{22}$ as determined by integrated ^{11}B NMR spectroscopy. This suggests that, at room temperature, the oxidative cluster dismantling procedure can occur with equal probability at either the B(9) or B(11) atom on the 11-vertex subcluster of anion **1**. However, the product isomer ratio is sensitive to the temperature. Integrated ^{11}B NMR spectroscopy showed that, at lower temperatures, 0 °C, a mixture of 60% *syn*-$B_{18}H_{22}$ and 40% *anti*-$B_{18}H_{22}$ is formed, and at higher temperatures, *ca.* 50 °C, the ratio is reversed.

The synthesis reported here of the 19-boron monoanion **1** begins with *syn*-$B_{18}H_{22}$, and therefore its deboronation to a 1:1 mixture of *syn*- and *anti*-isomers of $B_{18}H_{22}$ constitutes the first example of *syn*-$B_{18}H_{22}$ to *anti*-$B_{18}H_{22}$ isomer conversion. Published syntheses only exist for mixtures[14] of *anti*-$B_{18}H_{22}$ and *syn*-$B_{18}H_{22}$ or for *anti*-$B_{18}H_{22}$ only,[25−27] but no scheme has yet been found for the formation of isomerically pure *syn*-$B_{18}H_{22}$. However, synthesis of **1** using the procedure of Dopke et al., from *anti*-$B_{18}H_{22}$, followed by a subsequent deboronation of **1**, as described here, would effect a useful route for *anti*-$B_{18}H_{22}$ to *syn*-$B_{18}H_{22}$ conversion, and it thus represents a potentially useful method for *syn* isomer enrichment of $B_{18}H_{22}$.

A further noteworthy feature in compounds **1a** and **2a** is in the formation of the boronium cation $[PS\{BH_2\}]^+$ in the reaction. Such boronium cations, stabilized by monodentate or polydentate amine ligands and paired with a borane cluster anion such as in $[H_2B[N(CH_3)_2C_2H_5]_2[B_{12}H_{12}]$ or

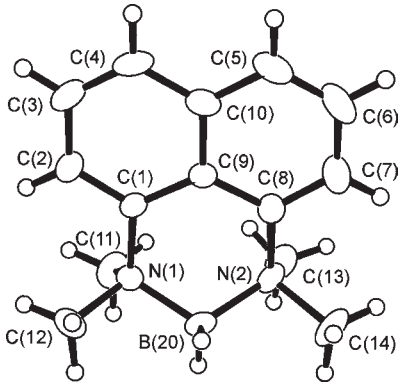

Figure 4. Representation of the crystallographically determined molecular structure of the cation $[C_{10}H_6(NMe_2)_2BH_2]^+$ in $[C_{10}H_6(NMe_2)_2BH_2][B_{19}H_{22}]$ **1a** (50% probability thermal ellipsoids). Selected distances (in Å) to N(1): B(20) 1.5964(18), C(1) 1.4789(16), C(11) 1.5064(18), C(12) 1.5094(18); to N(2): B(20) 1.595(2), C(8) 1.4795(17), C(13) 1.5086(17), C(14) 1.5083(16). Angles (in deg): N(1)B(20)N(2) 112.12(10), B(20)N(1)C(11) 113.65, (11)-B(20)N(1)C(12) 103.13(11), B(20)N(2)C(13) 114.98(11), B(20)N(2)C(14) 103.08(11), B(20)N(1)C(1) 111.89(10), B(20)N(2)C(8) 110.99(10).

the $[PSBH_2][B_2H_7]$ salt, have long been recognized.[29−31] However, this is the first structural characterization of the [1,8-bis-(dimethylamino)naphthalene(BH_2)]$^+$ boronium cation (Figure 4). These types of compounds may be formed from the reflux of diborane, B_2H_6, with amine ligand precursors; in the present work, it may be noted that diborane is formed in refluxing solutions of $BH_3(SMe_2)$.

Conclusion

A new, convenient, high-yield route to the nonadecaborate system is described. Both monoanionic $[B_{19}H_{22}]^-$ and dianionic $[B_{19}H_{21}]^{2-}$, compounds **1** and **2**, were experimentally characterized by single-crystal X-ray diffraction analysis and thereby provide a definitive solution to the question proposed by Jemmis et al. regarding the missing hydrogen atoms in the nonadecaborate anions first described by Dopke et al. Additionally, a method for the controlled cluster dismantling of **1** leading to mixtures of *syn*- and *anti*-$B_{18}H_{22}$ isomers, is described. As **1** was made from *syn*-$B_{18}H_{22}$, this is the first example of *syn*-$B_{18}H_{22}$ to *anti*-$B_{18}H_{22}$ isomer conversion. If used in conjunction with the synthesis of **1** from *anti*-$B_{18}H_2$ as described by Dopke et al., then the dismantling to give a *syn*- and *anti*-$B_{18}H_{22}$ mixture constitutes a useful new method for the formation of the *syn* isomer, or for *syn* enrichment of a *syn*- and *anti*-$B_{18}H_{22}$ mixture.

Experimental Section

All experiments were carried out in an ambient atmosphere unless otherwise stated. *syn*-$B_{18}H_{22}$ was synthesized by the literature method.[14] Proton Sponge (1,8-bis-(dimethylamino)naphthalene), borane-dimethyl sulfide complex, and 1,2-dichloroethane solvent were purchased from Aldrich Chemical Co. and used as received. NMR spectroscopy was performed at 9.4 T on a Varian MERCURY 400 High Resolution System. High resolution mass spectrometry, HRMS, was carried out on a Finnigan Fleet instrument using electrospray ionization using a CH_3CN solvent.

Synthesis of $[B_{19}H_{21}][PS\{BH_2\}]_2$ (2a). *syn*-$B_{18}H_{22}$ (0.22 g, 1 mmol) and Proton Sponge (2.2 g, 10 mmol) were placed together in a 50 mL 2-necked round-bottomed flask containing a magnetic stir bar. Under a flow of N_2 gas, 1,2-dichloroethane (15 mL) was added, and the resultant yellow solution was allowed to stir at room temperature under a stream of N_2(g) for 15 min. ^{11}B and ^{1}H NMR spectroscopic measurements of a sample of the yellow solution confirmed the complete formation of [*syn*-$B_{18}H_{21}$][PSH]. $BH_3(SMe_2)$ (0.77 g, 0.95 mL, 10 mmol) was then injected into the mixture, and the stirring continued at room temperature for a further 20 min. The temperature was then raised to 72 °C (± 1 °C), and the mixture stirred at this temperature for approximately 16 h. During this time, $[B_{19}H_{21}][PS\{BH_2\}]_2$ **2a** precipitates (0.59 g, 0.87 mmol, 87%) as a yellow semicrystalline solid. The precipitate was collected by filtration, washed with 1,2-$Cl_2C_2H_4$, and dried in the air at room temperature. Multinuclear NMR studies revealed at this stage excellent levels of purity suitable for further use. For analytical purposes, crystals were obtained from CH_3CN/Et_2O solvent diffusion. The HRMS spectrum of **1a** shows a typical boron isotopomer envelope with a cutoff peak at m/z 231.3508 [231.3485 calcd], which is representative of the $[^{11}B_{19}H_{22}]^-$ anion.

Synthesis of $[B_{19}H_{22}][PS\{BH_2\}]$ (1a). Concentrated H_2SO_4 was slowly dripped into a stirred CH_2Cl_2 suspension (15 mL) of $[B_{19}H_{21}][PS\{BH_2\}]_2$ (0.59 g, 0.87 mmol) until complete dissolution occurred. At this point, stirring was discontinued and the top CH_2Cl_2 layer separated, reduced in volume by half, and layered with hexane to form light yellow crystals of $[B_{19}H_{22}][PS\{BH_2\}]$ (0.38 g, 0.84 mmol, 97%) by slow diffusion of the hexane into the dichloromethane solvent.

Synthesis of Mixtures of $[B_{19}H_{21}][PS\{BH_2\}]_2$ (2a) and $[B_{19}H_{22}][PS\{BH_2\}]$ (1a). Using the above procedure for the synthesis of **2a**, but with a 2-molar excess of Proton Sponge rather than a 10-molar excess as above and a 5-molar excess of $BH_3(SMe_2)$ rather than a 10-molar excess, led to the formation of a mixture of compounds **1a** and **2a** (approximately 60% **2a** and 40% **1a** by integrated ^{11}B NMR spectroscopy, combined yield 92%). Isolation of this mixture, dissolution into CH_3CN, and either (a) shaking with 0.5 M aqueous NaOH or (b) addition of CF_3COOH led to the formation of pure **2a** or **1a**, respectively.

Formation of *anti*-$B_{18}H_{22}$ and *syn*-$B_{18}H_{22}$ from $[B_{19}H_{21}][PS\{BH_2\}]_2$ (2a). To a suspension of $[B_{19}H_{21}][PS\{BH_2\}]_2$ (0.22 g, 0.32 mmol) in $CHCl_3$ was added concentrated H_2SO_4 (1 mL) to effect a complete dissolution of the solids (the ^{11}B NMR spectrum revealed a complete conversion of **2a** to **1a**), at which point a 36% water solution of CH_2O (0.5 mL) was added, producing discoloration of the reaction mixture and effervescence. After the effervescence stopped, the top $CHCl_3$ layer was separated, the solvent removed, and the $B_{18}H_{22}$ product extracted into boiling hexanes. Removal of the hexane gave white, semicrystalline $B_{18}H_{22}$ (0.066 g, 0.31 mmol, 96%). Addition of the formaldehyde at 0 °C results in an approximately 60% *syn*-$B_{18}H_{22}$ and 40% *anti*-$B_{18}H_{22}$ mixture of isomers, room temperature gives 50% *syn*-$B_{18}H_{22}$ and 50% *anti*-$B_{18}H_{22}$, and +50 °C gives 40% *syn*-$B_{18}H_{22}$ and 60% *anti*-$B_{18}H_{22}$, all as determined by integrated ^{11}B NMR spectroscopy.

Single-Crystal X-Ray Crystallographic Analyses. Crystal data for $[B_{19}H_{22}][PS\{BH_2\}]$ **1a**: $C_{14}H_{42}B_{20}N_2$, M = 454.70, yellow prism, 0.4 × 0.3 × 0.25 mm^3, monoclinic, space group $P2_1/c$ (No. 14), a = 12.8900(2), b = 17.7510(3), c = 11.9970(3) Å, β = 91.1980(12)°, V = 2744.44(9) Å^3, Z = 4, D_c = 1.100 g/cm^3, F_{000} = 960; Nonius KappaCCD area detector, Mo Kα radiation, λ = 0.71073 Å, T = 150(2) K, $2\theta_{max}$ = 55.0°, 50 670 reflections collected, 6295 unique (R_{int} = 0.037). The molecular structure was solved with SIR97[32] and refined with SHELXL-97.[33] Final GoF = 1.027, R1 = 0.0502, wR2 = 0.1302, R indices based on

(29) Shore, S. G.; Parry, R. W. *J. Am. Chem. Soc.* **1955**, *77*, 6084.
(30) Miller, N. E.; Muetterties, E. L. *J. Am. Chem. Soc.* **1964**, *86*, 1033.
(31) Keller, P. C.; Rund, J. V. *Inorg. Chem.* **1979**, *18*, 3197.
(32) Altomare, A.; Burla, M. C.; Camalli, M.; Cascarano, G. L.; Giacovazzo, C.; Guagliardi, A.; Moliterni, A. G. G.; Polidori, G.; Spagna, R. *J. Appl. Crystallogr.* **1999**, *32*, 115.
(33) Sheldrick, G. M. In *SHELX-97*; University of Göttingen: Göttingen, Germany, 1997.

5166 reflections with $I > 2\sigma(I)$ (refinement on F^2), 425 parameters, 0 restraints. Lp and absorption corrections applied, $\mu = 0.052$ mm^{-1}. CCDC 747585.

Crystal data for $[B_{19}H_{21}][PS\{BH_2\}]_2$ **2a**: $C_{28}H_{61}B_{21}N_4$, $M = 680.82$, colorless prism, $0.35 \times 0.27 \times 0.18$ mm^3, triclinic, space group $P1$ (No. 1), $a = 8.8508(18)$, $b = 10.575(2)$, $c = 11.461(2)$ Å, $\alpha = 81.11(3)$, $\beta = 81.85(3)$, $\gamma = 75.56(3)°$, $V = 1020.4(4)$ Å^3, $Z = 1$, $D_c = 1.108$ g/cm^3, $F_{000} = 362$; Mach3 Kappa-type 4-circle goniostat, Mo Kα radiation, $\lambda = 0.71073$ Å, $T = 150(2)$ K, $2\theta_{max} = 59.4°$, 28 061 reflections collected, 10 214 unique ($R_{int} = 0.0520$). The molecular structure was solved and refined with SHELXS-97 and SHELXL-97.[34] Final GoF = 1.050, R1 = 0.0601, wR2 = 0.1494, R indices based on 7722 reflections with $I > 2\sigma(I)$ (refinement on F^2), 542 parameters, 3 restraints. Lp and absorption corrections applied, $\mu = 0.057$ mm^{-1}. Absolute structure parameter = 4(2). CCDC 747586.

Computational Method. Calculations carried out in this study were performed using the Gaussian 98 and Gaussian 03 packages. Structures were initially optimized with the STO-3G* basis sets using standard *ab initio* methods.[35,36] The next level of optimizations, including frequency analyses to confirm the true minima, together with GIAO NMR nuclear-shielding predictions, were performed using the B3LYP functional,[37,38] with the 6-31+G(d,p) and Huzinaga TZP (denoted as II) basis sets. The final level of optimizations was carried out at a correlated level of theory (MP2) with the 6-31G(d) basis set. The GIAO NMR nuclear shielding predictions were performed on the final optimized geometries. GIAO NMR nuclear shielding predictions were performed both on the B3LYP and MP2 optimized geometries, and the computed ^{11}B shielding values were related to the $BF_3.OEt_2$ scale using the experimental $\delta(^{11}B)$ value of B_2H_6, +16.6 ppm, as a primary reference.[39]

Acknowledgment. We thank the Grant Agency of the Academy of Sciences of the Czech Republic (M200320904, KAN400480701 and IAA400320901) and the Ministry of Education, Youth and Sports (LC523) for financial support and Mgr. M Kvíčalová for assistance in mass spectrometry measurements.

Supporting Information Available: Listings of DFT calculated atomic coordinates; mass spectra for compounds **1a** and **2a**; Complete Table 2. DFT calculated and X-ray measured interatomic distances for the monoanion $[B_{19}H_{22}][PSBH_2]$ **1a** and the dianion $[B_{19}H_{21}][PSBH_2]_2$ **2a**; Table 4. Measured ^{11}B-$\{^1H\}$ chemical shifts together with calculated ^{11}B chemical shifts for $[B_{19}H_{21}][PSBH_2]_2$ **2a** with the open-face *endo* hydrogen atom fixed in (a) the BH(9) and (b) the BH(11) positions as well as the equal-weight average of these calculations.This material is available free of charge via the Internet at http://pubs.acs.org.

(34) Sheldrick, G. *Acta Crystallogr., Sect. A* **2008**, *64*, 112.

(35) Frisch, M. J.; Trucks, G. W.; Schlegel, H. B.; Scuseria, G. E.; Robb, M. A.; Cheeseman, J. R., Jr.; Vreven, T.; Kudin, K. N.; Burant, J. C.; Millam, J. M.; Iyengar, S. S.; Tomasi, J.; Barone, V.; Mennucci, B.; Cossi, M.; Scalmani, G.; Rega, N.; Petersson, G. A.; Nakatsuji, H.; Hada, M.; Ehara, M.; Toyota, K.; Fukuda, R.; Hasegawa, J.; Ishida, M.; Nakajima, T.; Honda, Y.; Kitao, O.; Nakai, H.; Klene, M.; Li, X.; Knox, J. E.; Hratchian, H. P.; Cross, J. B.; Bakken, V.; Adamo, C.; Jaramillo, J.; Gomperts, R.; Stratmann, R. E.; Yazyev, O.; Austin, A. J.; Cammi, R.; Pomelli, C.; Ochterski, J.; Ayala, P. Y.; Morokuma, K.; Voth, G. A.; Salvador, P.; Dannenberg, J. J.; Zakrzewski, V. G.; Dapprich, S.; Daniels, A. D.; Strain, M. C.; Farkas, O.; Malick, D. K.; Rabuck, A. D.; Raghavachari, K.; Foresman, J. B.; Ortiz, J. V.; Cui, Q.; Baboul, A. G.; Clifford, S.; Cioslowski, J.; Stefanov, B. B.; Liu, G.; Liashenko, A.; Piskorz, P.; Komaromi, I.; Martin, R.; Fox, D. J.; Keith, T.; Al-Laham, M. A.; Peng, C. Y.; Nanayakkara, A.; Challacombe, M.; Gill, P. M. W.; Johnson, B. G.; Chen, W.; Wong, M. W.; Gonzalez, C.; Pople, J. A. *Gaussian 98*; Gaussian, Inc: Wallingford, CT, 2004.

(36) Frisch, M. J.; Trucks, G. W.; Schlegel, H. B.; Scuseria, G. E.; Robb, M. A.; Cheeseman, J. R., Jr.; Zakrzewski, V. G.; Stratmann, R. E.; Burant, J. C.; Dapprich, S.; Millam, J. M.; Daniels, A. D.; Kudin, K. N.; Strain, M. C.; Farkas, O.; Tomasi, J.; Barone, V.; Cossi, M.; Cammi, R.; Mennucci, B.; Pomelli, C.; Adamo, C.; Clifford, S.; Ochterski, J.; Petersson, G. A.; Ayala, P. Y.; Cui, Q.; Morokuma, K.; Malick, D. K.; Rabuck, A. D.; Raghavachari, K.; Foresman, J. B.; Cioslowski, J.; Ortiz, J. V.; Baboul, A. G.; Stefanov, B. B.; Liu, A. L.; Piskorz, P.; Komaromi, I.; Gomperts, R.; Martin, R. L.; Fox, D. J.; Keith, T.; Al-Laham, M. A.; Peng, C. Y.; Nanayakkara, A.; Gonzalez, C.; Challacombe, M.; Gill, P. M. W.; Johnson, B.; Chen, W.; Wong, M. W.; Andres, J. L.; Gonzalez, C.; Head-Gordon, M.; Replogle, E. S.; Pople, J. A. *Gaussian 03*; Pittsburgh, 1998.

(37) Becke, A. D. *J. Chem. Phys.* **1993**, 5648.

(38) Lee, C.; Yang, W.; Parr, R. G. *Phys. Rev. B* **1988**, *37*, 785.

(39) Onak, T.; Tseng, J.; Diaz, M.; Tran, D.; Arias, J.; Herrera, S.; Brown, D. *Inorg. Chem.* **1993**, *32*, 487.